SEVEN
publicações acadêmicas

Study of the mechanical properties of repair of AISI 1020 steels with a composite based on polymeric adhesive and carbon fiber

Crossref doi
https://doi.org/10.56238/interdiinovationscrese-081

Felipe Roberto da Silva e Silva
Rio de Janeiro State University, FCEE/UERJ, RJ, Brazil

Silvana de Abreu Martins
Rio de Janeiro State University, FCEE/UERJ, RJ, Brazil

Arsitoclê Aguiar Filho
Technical School Support Foundation, FAETEC, RJ, Brazil

Gabriel Mário Guerra Bernadá
Fluminense Federal University, PGMEC/UFF, RJ, Brazil

Charles de Abreu Martins
ArcelorMittal - Global Research & Development, Avilés, Spain

ABSTRACT
Due to the great importance of steel in engineering and economics and the challenges related to its resistance to corrosion and high density, studying methods to extend its useful life becomes essential, avoiding failures in service or increased operational costs, like exchanging components, for example. Traditionally, in repairs of defects in steel, welding has been used. However, other methods have stood out, such as using adhesives and composites in repair, thanks to lower costs and greater operational ease. In this work, an experimental study of the repair of an AISI 1020 was carried out using a composite with structural adhesive based on epoxy and carbon fiber. A defect was caused in the machining laboratory through a 2mm hole in the entire thickness and a hole in half the thickness. A computer simulation was carried out to evaluate the effect and stress concentrations in the defect in AISI 1020 steel, which showed that the tensioned material begins to plasticize in the defect region. This confirmation was essential to validate the repair.
Furthermore, after the repair, tensile tests were carried out to evaluate the repair effects. Previously, the blasting was used to improve the adhesion of the composite to the surface since roughness enhances the anchoring of the adhesive. After a tensile test, the positive effect of the repair was verified.

Keywords: AISI 1020, Mechanical properties, Steel repair, Adhesive.

1 INTRODUCTION

In recent years, several methods of repairing steel with adhesives have been developed and proven to be efficient, in many cases being able to replace welding more economically, with reduced energy consumption, specialized labor and more, safely for operators, extending the useful life of a structure or pipeline. It can also be cited using steel printing technologies with promising results. The repair of steels using adhesives and composites, the effects of repairs, their efficiency and behavior have been the subject of study by many researchers. It can highlight the work of (PRAETZEL, 2020) on repair with composite in pressure vessels, the research of (PRAETZEL, 2021) on the effects of accelerated aging in composites used in the repair of pipes in the oil industry, and the study of the analysis of deformations in steel pipes repaired with composites (THOMAZI, 2013), the research by (ROHEM, 2021) on the development and qualification of a new laminated polymer matrix composite

for the pipe repair, and (LIA, 2020) on offshore steel pipes cracked on the external surface reinforced with a composite repair system and (MATTOS, 2021) who studied the long-term field performance of a composite pipe repair under hydrostatic pressure. Only a few were mentioned here, but many of these studies explore the most appropriate design, such as the thickness of the layers of adhesives and composites, preparation of the surfaces, and the pressure to which the repaired metal assembly will be subjected.

According to (OLIVEIRA, 2019), it is of great importance to master corroded pipeline repair technologies to reduce costs in the transportation of hydrocarbons, as loss of thickness caused by external or internal corrosion in used steel pipelines is almost inevitable in the land transport of oil and its derivatives. Therefore, some techniques for pipeline repair have been proposed over the years, such as the cut-and-replace technique. (SILVA, 2022) also, steel pipelines that transport oil and oil products on land suffer external or internal corrosion due to failures in cathodic protection or coating or the presence of moisture and water in the product. This corrosion reduces the thickness of the pipelines and increases the costs of transporting hydrocarbons. However, techniques such as cut and replace, double welded gutter, which surrounds the duct with two gutter halves and welds, and double filled gutter, which injects material between the duct and a sleeve, have some disadvantages. Such as the high cost due to operational downtime, risk of accidents and repair delays. Therefore, new repair techniques are being researched to improve efficiency and reduce costs. Among such techniques, we can mention the use of adhesives and composites. The oil and gas industry has widely used fiber composite reinforcing adhesives to repair underwater structures. However, it is necessary to evaluate the most suitable types of adhesives and reinforcements and the parameters and the relationship at the interface between the metal and repair phases. Furthermore, it is essential to evaluate the repair system, mainly using computational prediction models capable of providing information about repair performance. Motivated by the need for research into repair techniques, this work used a structural adhesive and carbon fiber fabric repair on AISI 1020 steel repair, presenting a positive result.

2 MATERIALS AND METHODS

Materials used in this work will be described below, as well as the methodology used in this research. This methodology involves Planning, Sample preparation, Steel, computer simulation and Tensile tests.

2.1 MATERIALS

The following materials were used in this work:

- AISI 1020 steels;
- Medium fluid epoxy-based structural adhesive;

- G18 TH Shot;
- Carbon Fiber Fabric;
- Spatula;
- Brush;
- Personal protective equipment (PPE) and fume hood.

2.1.1 Description of Materials

2.1.1.1 Steels

In this work, samples of two steels was used, AISI 1020 with a thickness of 4mm (5⁄32"). This material was donated in the form of a plate to be worked on, as shown in figure 1.

Figure 1 – 1020 Steel Plate used in this research, as received. Source: The author, 2023

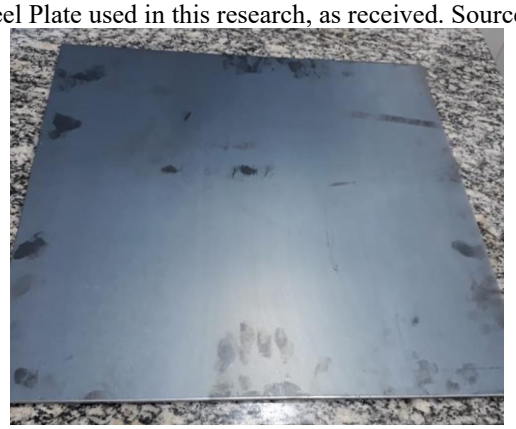

To carry out the tests, the AISI 1020 steel specimens were also cut following the ASTM A370 standard.

2.1.2 Structural adhesive

Table 1 describes the structural adhesive used in this work, based on medium fluid epoxy.

Table 1 - Description of the structural adhesive used. Source: The author, 2023.

Product	Structural Adhesive
Use of Waterproofing	to Repair and Protect Structures
Yield Information	1 kg can (A+B) - 0.55 m²
Drying Time	0.83 h
Observations on Drying	Maximum 50 minutes, at a temperature of 25°C
Recommended Use	Anchors, anchors, iron, stone, ceramics.
Color	Gray color
Finish	Smooth
Height	20.00 cm
Width	11.00 cm
Product Weight	1.0 g

2.1.3 Other materials

Shot blasting, Carbon Fiber Fabric for reinforcement; Spatula; Brush, Personal Protective Equipment (PPE), acetone and fume hood are described below:

2.1.3.1 hot blasting

In the process of adhering the metallic material to the composite, a steel shot blasting step was necessary, causing it to gain greater roughness on the surface in contact with the adhesive, making better adhesion possible. Figure 2 refers to the shot blasting sample used in the process.

Figure 2 – Shot blasting G18 TH and Lot: 262483208. Source: The author, 2023.

2.1.3.2 Carbon Fiber

It is used to reinforce 45-degree bidirectional carbon fiber fabric as reinforcements for the adhesive. These reinforcements were chosen based on literature and suggestions from steel suppliers. Figure 3 shows the carbon fiber applied in the repairs.

Figure 3 –Carbon fiber fabric used in this work. Source: The author, 2023.

In addition to the materials mentioned above, a metal spatula with a wooden handle, a small brush for homogenizing and distributing the adhesive on the samples, and acetone were used to clean them. PPE, gloves, mask, safety glasses, and lab coat were used, and the adhesive was handled inside the fume hood to avoid inhaling organic vapors and odors from the adhesive, as shown in figure 4.

Figure 4 - Handling of the adhesive was carried out inside the fume hood. Source: The author, 2023

3 METHODOLOGY

The damage caused was two types of holes, going through the entire thickness of the material and holes up to 50% of the thickness of the steel samples. Figure 5 shows a sample. To repair the defect caused in the steel samples, a medium fluid epoxy-based structural adhesive was used, adding carbon fiber fabric for reinforcement with a bidirectional weave at 45 degrees.

Figure 5 - Damage caused, holes going through the entire thickness. Source: The author.

The fiber was added to promote greater resistance, and the two types of repairs, with carbon fiber in a hole going through the thickness of the sample and up to 50% of the thickness, were compared, analyzing the location and conditions of fracture in tension and determining the properties. The hardness test is used to evaluate and prove the identification of steel since steel with a higher carbon content has greater hardness.

The adhesive used consists of two components, the resin (component A) and the hardener (component B), with its mixing ratio already defined and separated on the packaging by the manufacturer, and the user is only responsible for mixing with the total material contained in the packaging. The packaging supplied had 0.5 kg of resin and 0.5 kg of hardener, with the technical characteristics being available on the product packaging.

After machining, the metal's surface presented a mirrored appearance due to the cutting tool, which gave a surface finish with lower roughness than was necessary for the experiment. This step had to be corrected with another blasting stage, where the pieces gained a good anchoring surface for the adhesive and carbon fiber. To prepare the samples, machining cutters were used to create the profile of the traction body according to ASTM A370 standards.

Part of the tensile tests was carried out at the company CMBA Indústria Mecânica LTDA with the assistance of the company's laboratory specialist, where it was used in a WOLPERT universal testing machine with a load cell of 200 KN or approximately 20000 kgf, and also used as a reference test to ASTM A370, where the test speed was: 5mm/min on the 4mm thick AISI1020 sample repaired with the composite. The other part of the tensile test was carried out at LAMAT – Materials laboratory at the Celso Suckow da Fonseca Federal Center for Technological Education (CEFET/RJ) of Maracanã, where an INSTRON universal testing machine with a load cell of 200 KN or approximately 20000 kgf was used.

The AISI 1020 steel samples with defects, as mentioned previously, in the form of holes produced with different thicknesses up to 50% and holes up to 100%, crossing the entire thickness with a 2mm diameter drill. The material's substrate surface was prepared at the Industrial Processes and Nanotechnology Laboratory (LPIN), at the State University of Rio de Janeiro on the West Zone Campus of Rio de Janeiro (UERJ-ZO).

Acetone was used to remove impurities, such as oil, grease, and dirt, among others, and to clean the metal surface. The adhesive consists of two components (A and B) which come in cans joined by a plastic strip and which, once the packaging is opened, are mixed and must be homogenized using a spatula or mechanical mixer until obtaining a grey color, according to the manufacturer's instructions. Using a brush, the adhesive was applied to the defect region with a layer of approximately 1mm, a layer of fiber, fabric was applied to the adhesive, and then another layer of adhesive and another layer of fiber were applied. Figure 6 shows the fiber application process.

Figure 6 - Application of the adhesive together with the carbon fiber. Source: The author, 2023.

Despite the small size of the hole, it was decided to apply the adhesive over a wide area to better 'hold' the region around the hole, providing greater security in the repair, with a total of two layers of adhesive and two layers of fiber. Figure 7 shows the Application of the adhesive together with the carbon fiber on the other layers. The adhesive used has a relatively short pot life, becoming extraordinarily viscous and difficult to apply after approximately 20 to 30 minutes.

Figure 7- Application of the adhesive together with the carbon fiber on the other layers. Source: The author, 2023.

However, the samples remained in the fume hood for fourteen days until the tensile tests were carried out, ensuring a recommended curing time. Aiming to qualitatively analyze the stress state in the samples to be experimentally tested, a computational simulation was carried out using the finite element analysis software COMSOL Multiphysics, considering an approximate geometry as shown in Figure 8. A hole is placed in the center of the specimen to simulate a defect that creates brittleness, where the crack begins during loading, as has been performed experimentally. A mixed-mode fracture is induced by displacing the hole and notch from the center of the plate. The load is applied through metal pins with controlled displacement inserted into a small hole. The model assumes a plane stress condition.

Figure 8 – Representation of the specimen mesh analyzed by computer simulation, (above) and zoom of the mesh of the stress concentrators considered, through and non-through holes (below). Source: The author, 2023

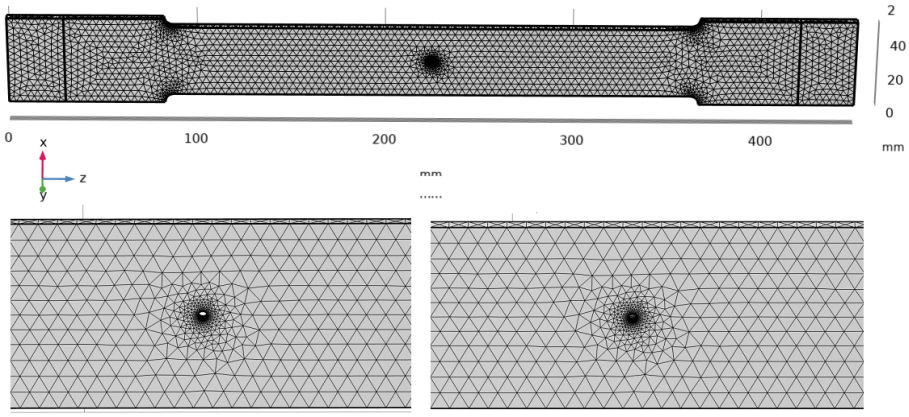

The results of the equivalent Von Mises stresses for the cases analyzed are presented below. Figures 9 and 10 show the state of stress in the test tube and the region of the through-hole stress concentrator, highlighting in red the maximum stresses reached in the test. Figure 11 shows the displacement field of the bar considering the left end with zero displacement and the right side with an imposed displacement of 30mm

Figure 9 – Von Mises stress field in the AISI 1020 beaker, and zoom in on the stress concentrator zone (below) of the sample with a hole up hole, according to COMSOL MultiPhysics V4.4. Source:The author, 2023.

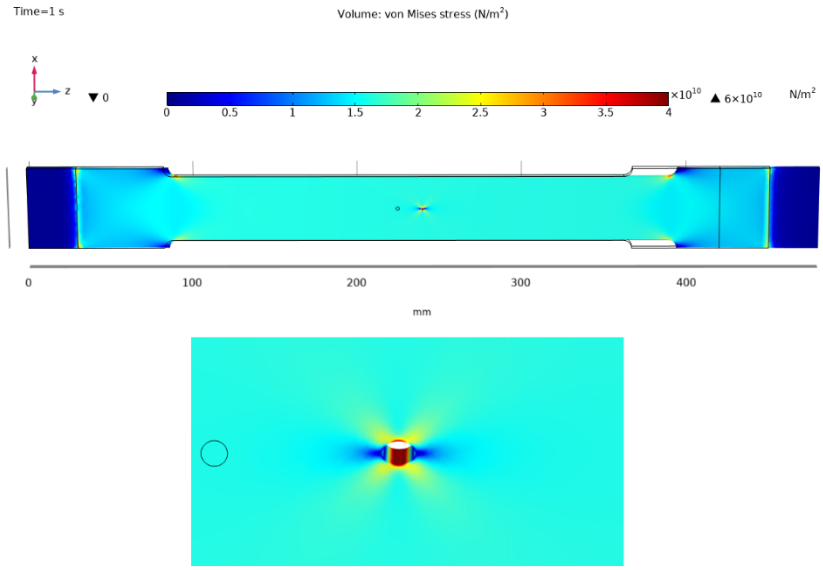

Figure 10 - Von Mises stress field in the sample, and zoom in on the stress concentrator zone (below) of the sample with a hole up to half the thickness in the sample, according to COMSOL MultiPhysics V4.4. Source: The author, 2023.

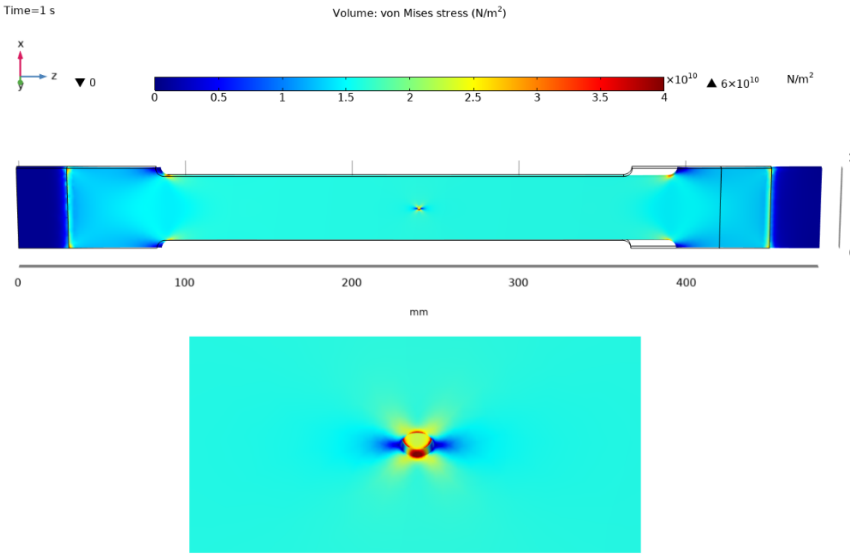

Figure 11 – Specimen displacement field where the blue part refers to zero and the red part is the maximum 30mm of displacement, and zoom in on the stress concentrator area (below). Source: The author, 2023.

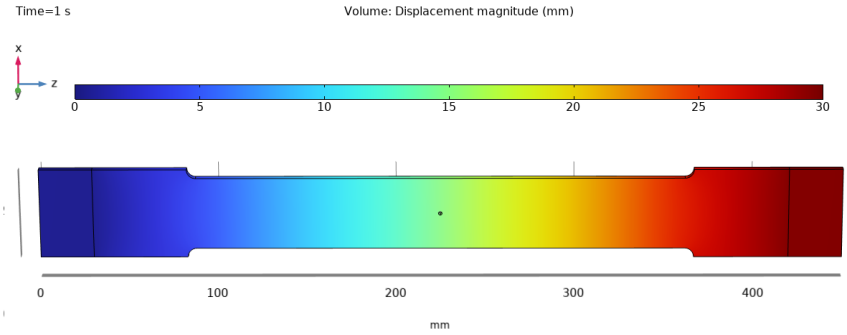

From the results obtained, both samples show that the maximum stress zones were in the center of the stress concentrators, where most of the reddish region is concentrated. According to the simulation, these show that the added defects generate a concentration of stresses where the material reaches failure stresses (plasticization) and can give rise to cracks in this critical region for the initiation of failure.

The next example studies the fracture of specimen in the model, including dimensions and material properties as the plate is loaded, a mixed-mode fracture is induced with a crack propagating from the predefined placed hole in the center. Fracture is modeled using a damage model that regularizes the sharp geometry of the crack by the phase field approximation. This means that the crack is described in the domain material, so the non-local phase field makes the crack path independent of the mesh elements. The example shows how to define an efficient and stable solver configuration for the phase field damage method.

Figure 12 presents the results of the numerical modelling that describes the fracture process in the elastic body from its nucleation to the propagation and branching of cracks.

Figure 12 - Crack phase field evolution for different step times. Source: The author, 2023

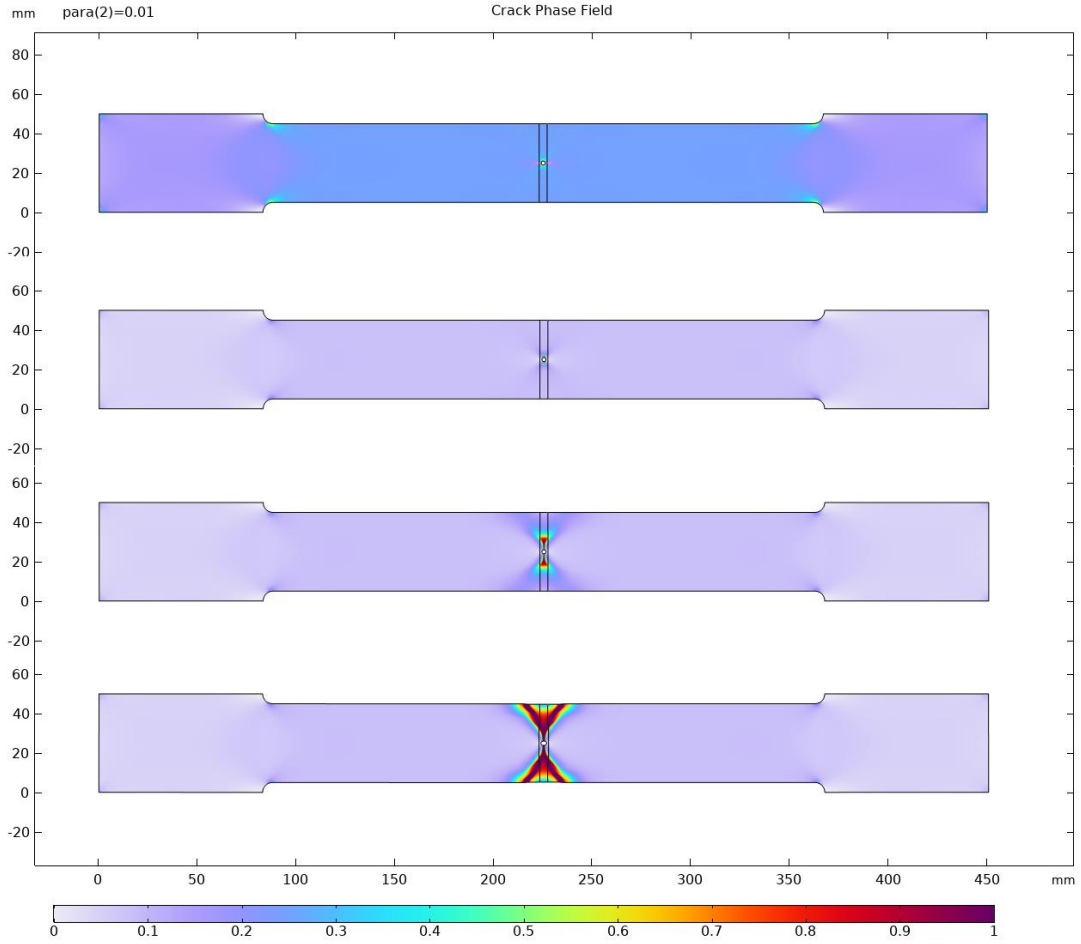

4 RESULTS

Figure 13 shows the sample without repair fractured and sample repaired. Fractured fixed in the tensile machine, and it is possible to observe that the fracture happened outside of the area where the hole was made and repaired. Therefore, out of the repair area.

Figure 13 - Fractured sample, right, without repair and left fixed in tensile machine after testing, repaired with composite. Source: The author, 2023.

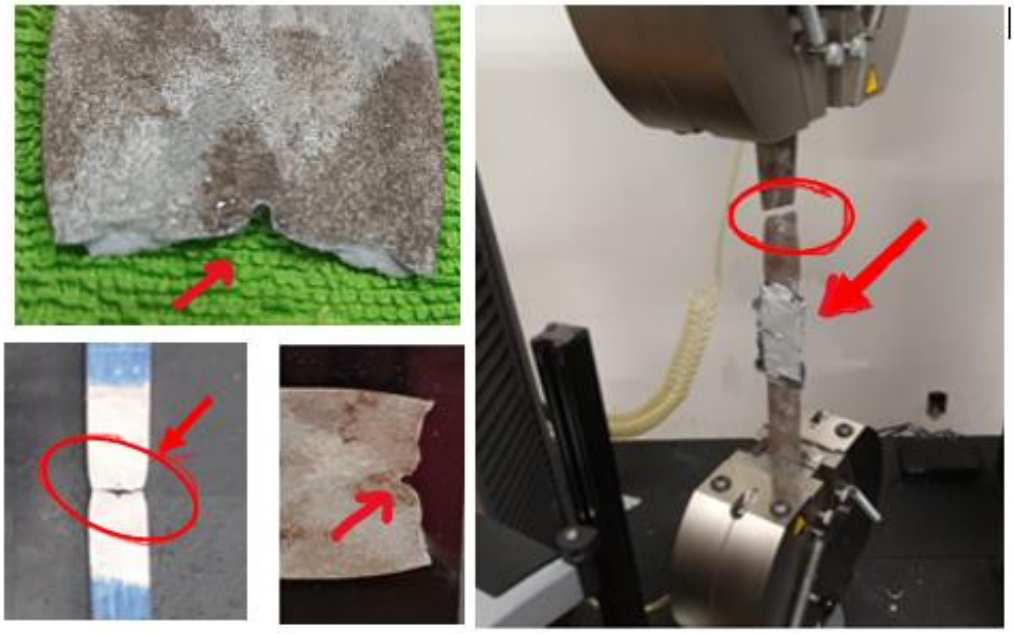

Tables 3, 4 and 5 present the results of the tensile tests. Table 3 shows the test results of the without defect samples carried out only at the CMBA company. The operator of the traction machine determined the test speeds in the steel tests due to the machine's operating conditions. While Table 4 shows the results of the samples tested with a defect and a repaired defect, carried out in the CEFET laboratory (Maracanã) and the mechanical testing laboratory at the company CMBA, the operator also defined the differences in test speed between the samples, due to the condition of the equipment. In any case, using different speeds was interesting, as it added additional information: the effect of the difference in speed on the test. Table 5 presents an analysis of defective and repaired samples.

Table 3 - Analysis of samples without defects, test carried out. Source: The author, 2023.

Sample	Test speed mm/min	Load Endurance limit (Kgf)	Stress Endurance limit (MPa)	Yield limit (MPa)	Elongation (%)
CMBA (AISI 1020)	5	7323	386.5	308.1	30.0
CMBA (AISI 1020)	5	6436	389.3	297.6	26.5

Table 4 - Analysis of samples without defects, average value, test performed. Source: The author, 2023.

Sample	Test speed (mm/min)	Strength limit (MPa)	Yield limit (MPa)	Elongation (%)
Steel (AISI 1020)	5	387.9	302.9	28.3

Table 5 - Analysis of defective and repaired samples. Source: The author, 2023.

Sample	Test speed (mm/min)	Load Resistance limit (Kgf)	Strenght Limit (MPa)	Yield limit (MPa)	Elongation (%)	Observation (Where the sample broke)
(AISI 1020) Through hole with CEFET repair	3	5810.5	333.9	250	21%	In steel
(AISI 1020) Hole 1/2 thickness with CEFET repair	5	5848.5	356.6	275	25.5%	In steel
(AISI 1020) Unrepaired through hole CMBA	5	6452	400.6	332	17.3%	In the hole

Figure 14 presents a general flowchart with the main stages of this work, such as receiving steel samples, creating the defect using machining, repair with the composite, tests and test results.

Figure 14 – flowchart general, with the main stages of this work. Source: The author, 2023.

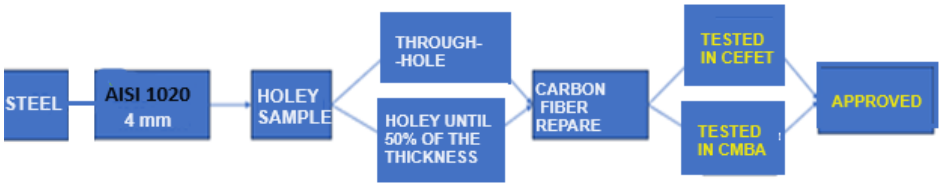

5 DISCUSSION OF RESULTS

In the simulation of the stress state in AISI 1020 steel, using the COMSOL Multiphysics V4.4 software, it can be observed that the defect, caused in the 1020 steel samples, was effective in the sense of being the place where plasticization and rupture of the samples. This was important to observe the effect of the repair on the samples.

In the tensile test itself, the results considering the specimens without defect, with defect and with repaired defect, it is clear that:

- In samples with defects and repaired defects, there was a tendency for the defect to reduce the resistance and yield limit of the samples, as well as elongation.
- The test speed influenced the 1020 steel, increasing both the resistance and yield limits with the increase in the test speed, as expected since it is a high ductility of steel.
- The fracture region in the tensile test was the main element that demonstrated the effect of the defect and the repair. Therefore, observing the samples, it is clear that the rupture was outside the repaired defect, but in the one without repair, it has occurred in the defect. The preparation conditions were good due to its roughness; the adhesive was applied when

it still had greater fluidity, ensuring more excellent wettability, in addition to the fact that it was thinner, facilitating the penetration of the adhesive throughout the hole.

6 CONCLUSIONS

It can be concluded that:

- The epoxy-based structural adhesive associated with the fibers effectively repaired the defect caused in the AISI 1020 steel samples since the rupture of the test piece occurred in a region outside the repair area.
- As a 2mm diameter hole under tension, the defect was the point at which plasticization began, observed in experimental tests and by computer simulation.
- The fracture region was the most significant evidence of the effect of the repair on the steel and its effectiveness due to the fracture occurring outside the defect region after the repair.
- The influence of the tensile test speed was evident, showing that a higher speed results in higher resistance and yield limits.
- The numerical models presented qualitative results similar to the experimental results. Therefore, once calibrated, they could become an effective tool for predicting fracture behavior.

ACKNOWLEDGMENT

The authors would like to thank the Solid Mechanics Laboratory at COPPE/UFRJ for access to the COMSOL MultiPhysics V4.4 license, to Professors Humberto Nogueira Farneze and Luís Felipe G. de Souza from the Federal Center for Technological Education Celso Suckow da Fonseca- CEFET/RJ. They also thank the company ArcelorMittal for donating the steel sheet, to the machining technician Cynthia, Eric Tiago Neiva and the company CMBA Indústria Mecânica LTDA, Luciano de Lima Paulo, Rubem Antônio dos Santos and Fernando Ferreira de Oliveira.

REFERENCES

LIA, Zongchen et al. External surface cracked offshore steel pipes reinforced with composite repair system subjected to cyclic bending: An experimental investigation. Theoretical and Applied Fracture Mechanics, Amsterdam, v. 113, p. 1-13, June, 2020.

MATTOS, H.S. da C. et al. Long-term field performance of a composite pipe repair under constant hydrostatic pressure. Engineering Failure Analysis, Amsterdam, v. 125, p. 1-12, June, 2021.

OLIVEIRA, Henrique de. Estudo do comportamento em fratura de materiais compósitos para reparo de dutos de aço. 2019. 120 f. Dissertação (Mestrado em Engenharia Mecânica) – Universidade Federal do Rio de Janeiro, Rio de Janeiro, 2019.

PRAETZEL, Rodrigo et al. Accelerated aging effects in composites used as repair for pipes in oil industry. Polymer Composites, Hoboken, v. 42, n. 9, p. 1-10, Sep., 2021. Disponível em: https://doi-org.ez393.periodicos.capes.gov.br/10.1002/pc.26271. Acesso em: 25 out. 2021.

PRAETZEL, Rodrigo et al. Monitoring the evolution of localized corrosion damage under composite repairs in pipes with guided waves. Journal of Pressure Vessel Technology, New York, v. 142, n. 6, p. 1-9, Dec., 2020.

ROHEM, N.R.F. et al. Development and qualification of a new polymeric matrix laminated composite for pipe repair. Composite Structures, Amsterdam, v. 268, p. 1-11, June, 2021.

SILVA, A. C. et al. Influência da temperatura de soldagem na microestrutura e na resistência à corrosão de juntas soldadas de aço inoxidável superduplex UNS S32750. Tecnologia em Metalurgia, Materiais e Mineração, v. 7, n. 2, p. 60-66, 2010. Disponívelem: https://tecnologiammm.com.br/article/10.4322/tmm.00302010/pdf/1573492069-3-2-60.pdf. Acesso em: 6 mai. 2022.

THOMAZI, Cinthia T. C. L.; LEVY NETO, Flaminio. Análise das deformações em tubos de aço reparados com compósitos tipo carbono/epóxi. Soldagem & Inspeção, São Paulo, v. 18, n. 4, p. 36.